# Magnetic Properties of $KMnF_3$. II. Weak Ferromagnetism*

A. J. HEEGER,† OLOF BECKMAN,‡ AND A. M. PORTIS
*University of California, Berkeley, California*

(Received April 24, 1961)

The static magnetic properties of single-crystal $KMnF_3$ have been studied by magnetic torsion measurements. These measurements are consistent with a transition to uniaxial antiferromagnetism below 88.3°K. Below 81.5°K the magnetic behavior is complex with the development of hysteresis and discontinuities in the torsion. Further, the torsion increases linearly with magnetic field in this range. These observations suggest the development of weak ferromagnetism in this crystal below 81.5°K. From a comparison of the direction of the weak moment and the known distortions in the crystal structure it is concluded that the weak moment results from a canting of the magnetic sublattices because of differences in the sublattice anisotropy. Between 81.5° and 88.3° a moment appears only in strong magnetic fields. It is shown that the moment is developed in a field because of the increased parallel susceptibility of a canted antiferromagnet. The canting transition is interpreted as a first order transition of the Jahn-Teller type. The antiferromagnetic transition itself is associated with a change in lattice parameter and is interpreted as an exchange-controlled first-order transition.

## I. INTRODUCTION

FROM measurements of the static magnetic susceptibility of polycrystalline $KMnF_3$ as a function of temperature[1,2] it has been generally concluded that this crystal becomes antiferromagnetically ordered below 88.3°K. Accurate measurement of the temperature dependence of the shift in the $F^{19}$ nuclear resonance[3] indicates a susceptibility of the form $\chi=C/(T+\theta)$, with $\theta=238$°K. From the magnitude of the resonance shift and its directional dependence and from the small resonance linewidth a strong superexchange interaction between manganese ions seems indicated. The resonance was observed to broaden and decrease rapidly in intensity as the temperature was reduced to 88.3°K, suggesting an antiferromagnetic transition. The continuity of the magnetic susceptibility and its temperature independence just below the transition supports this interpretation. Recent neutron diffraction studies of powdered $KMnF_3$ have confirmed[4] the existence of antiferromagnetic ordering at low temperatures. The $Mn^{2+}$ ions lie on a simple cubic lattice and the neutron studies indicate that the spins are ordered so that the spin directions alternate along a cube edge. It was not possible however to determine the orientation of the spins with respect to the crystal.

The behavior of the static magnetic susceptibility of $KMnF_3$ above its magnetic transition and down to about 10 deg below the transition is that of a classic antiferromagnet. But below 81.5°K the static magnetic measurements indicate a highly nonlinear magnetic susceptibility.[2,5] Measurements in this laboratory of the magnetic anisotropy of single crystals of $KMnF_3$[6] gave independent indication of a second transition at this lower temperature. These measurements, which are described in detail here, establish that the observed nonlinear behavior is associated with the development of a weak ferromagnetic moment as the result of a slight canting of the sublattice moments.

A theory of the relation between canted antiferromagnetism and crystal symmetry has been developed by Dzialoshinskii[7] with special application to the weak ferromagnetism of $\alpha$ $Fe_2O_3$. Bozorth[8] has developed a theory along similar lines with special application to the rare earth orthoferrites. This theory has been extended by Moriya[9,10] with emphasis on the physical interactions responsible for canting. Moriya points out that there are two distinct mechanisms which can produce canting. One mechanism is a difference in the single-spin magnetocrystalline anisotropy for differing sites.[9] These differences could produce differing anisotropy at the two sublattices. Since a small canting will lower the anisotropy energy in first order while it raises the exchange energy only in second order, canting will be expected where it is consistent with the symmetry. The second mechanism is associated with the exchange coupling itself.[10] Moriya has demonstrated that for certain symmetries there may be an antisymmetric exchange coupling which will lead to canting. The crystal structure of $KMnF_3$ has been studied in order to determine the symmetry of the $Mn^{2+}$ sites.[11] The crystal is found to be

* Supported by the U. S. Atomic Energy Commission.

† National Science Foundation Cooperative Fellow.

‡ On leave from Uppsala University, Uppsala, Sweden. Appointment supported by the International Cooperation Administration under the Visiting Research Scientists Program administered by the National Academy of Sciences of the United States of America.

[1] R. L. Martin, R. S. Nyholm, and N. C. Stephenson, Chem. & Ind. (London) **1956**, p. 83; Shinji Ogawa, J. Phys. Soc. Japan **14**, 1115 (1959).

[2] Kinshiro Hirakawa, Kazuyoshi Hirakawa, and Takasu Hashimoto, J. Phys. Soc. Japan **15**, 2063 (1960).

[3] R. G. Shulman, K. Knox, and B. J. Wyluda, Bull. Am. Phys. Soc. **4**, 166 (1959). R. G. Shulman, and K. Knox, Phys. Rev. **119**, 94 (1960).

[4] V. Scatturin, L. Corliss, N. Elliott, and J. Hastings, Acta Cryst. **14**, 19 (1961).

[5] Shinji Ogawa (private communication).

[6] O. Beckman, A. J. Heeger, A. M. Portis, and D. T. Teaney, Bull. Am. Phys. Soc. **5**, 188 (1960).

[7] I. E. Dzialoshinskii, J. Exptl. Theoret. Phys. U. S. S. R. **32**, 1547 (1957) [translation: Soviet Phys.—JETP **6**, 1130 (1958)]; J. Phys. Chem. Solids **4**, 241 (1958).

[8] R. M. Bozorth, Phys. Rev. Letters **10**, 362 (1958).

[9] Toru Moriya, Phys. Rev. **117**, 635 (1960).

[10] Toru Moriya, Phys. Rev. **120**, 91 (1960).

[11] Olof Beckman and Kerro Knox, Phys. Rev. **121**, 376 (1961), referred to as I.

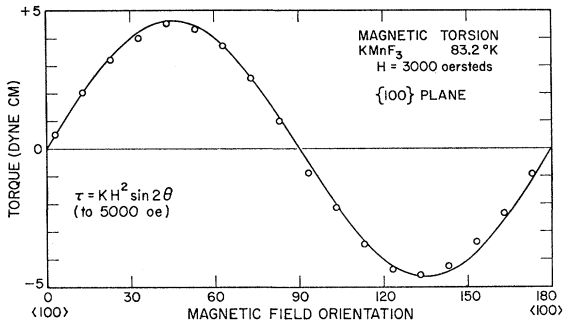


FIG. 1. Magnetic torsion of a single crystal of $KMnF_3$ at 83.2°K in the uncanted state for a field in the {100} plane. The torque is observed to vary as the square of the field and with a period of 180°.

distorted from its perovskite structure with the probable space group $Pbnm$ ($D_{2h}^{16}$). As will be shown below the indicated structure suggests a single-ion anisotropy of a form leading to canting. Pearson[12] has examined the sources of single-ion anisotropy in the distorted structure and finds that the observed fluorine displacements should produce a distortion of the $Mn^{2+}$ spherical dipole distribution. Estimates of the expected distortion are in good agreement with the observed anisotropy energies. It is believed therefore that the canting observed in $KMnF_3$ is primarily associated with the anisotropy of the dipolar energy of the $Mn^{2+}$ core and that there is very little orbital coupling of the kind that would result in antisymmetric exchange.

## II. EXPERIMENTAL RESULTS

The anisotropy of the magnetic susceptibility of a single crystal[13] of $KMnF_3$ was investigated by torsion measurements in a uniform magnetic field. The apparatus is similar to that previously described by Stout.[14] The crystal is rigidly attached to a long glass rod, which is connected via the suspension wire to the rotating torsion head. A mirror, fixed on the rod, determines the orientation of the crystal. By rotating the torsion head until the mirror is back to its zero-field position, the torque is determined for a particular orientation of the magnetic field with respect to the crystal. In discussing the experimental results we will distinguish three temperature regions: (1) above 88.3°K—paramagnetic region, (2) between 88.3° and 81.5°K—uniaxial antiferromagnetic region, and (3) below 81.5°K—canted antiferromagnetic region.

In the temperature range above 88.3°K there was no detectable anisotropy in the magnetic susceptibility. Even though the crystallites are tetragonally distorted[11,15] the samples are highly twinned so that if the tetragonal axes are equally distributed over the cube directions, no torque should be observed in a field. Below 88.3° a small torque is developed. For a uniaxial antiferromagnet we expect[16]

$$\tau = (\chi_\perp - \chi_{||}) H^2 \sin 2\theta,$$

where $\theta$ is the angle between the field direction and the magnetic axis. One expects from molecular field theory that $\chi_\perp = 1/\lambda = \chi(T_N) \sim 1.5 \times 10^{-2}$ per mole and $\alpha = 1 - \chi_{||}/\chi_\perp \sim (T_N - T)/T_N$ near $T_N$. Then the maximum torque per mole should be about $1.7 \times 10^{-4} H^2 (T_N - T)$. The sample weighed 390 mg or 0.0026 mole. The observed torque as shown in Fig. 1 follows this law except that the torque is only 10% of the indicated magnitude. The observed reduction follows from the twinning and is not unexpected. The dependence of the torque on field at 83.2°K for fields up to 7000 oe as shown in Fig. 2. A plot of $\alpha$ as a function of temperature is shown in Fig. 3. It can be seen that the torque is accurately proportional to $H^2$. For fields above 7000 oe the sample behavior becomes surprisingly complex. For the crystal suspended

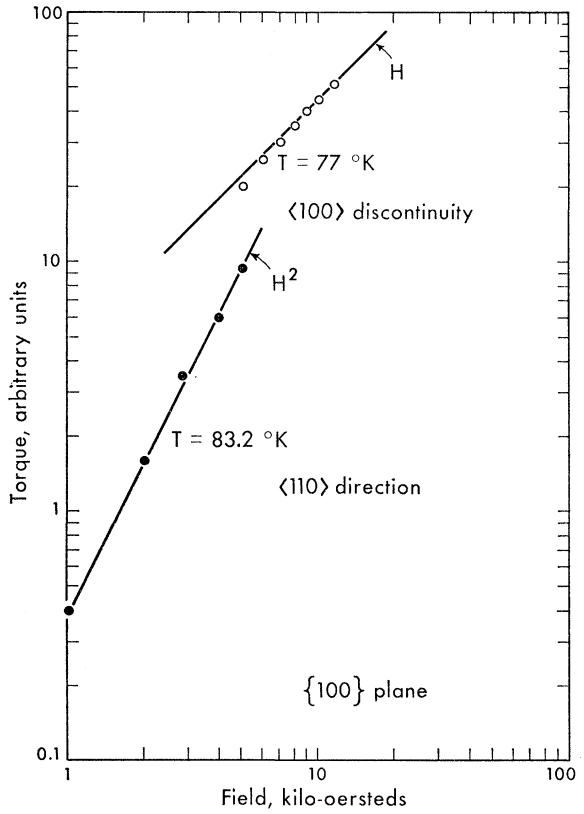


FIG. 2. Plot of the torque at 83.2°K in the uncanted state demonstrating that the torque is accurately proportional to $H^2$. At the top of the figure is shown the magnitude of the ⟨100⟩ discontinuity in the torque as a function of field. The discontinuity is proportional to the field at high fields.

[12] J. J. Pearson, Phys. Rev. **121**, 695 (1961).
[13] We are indebted to Dr. Kerro Knox of the Bell Telephone Laboratories for preparing this crystal and making it available to us.
[14] J. W. Stout and M. Griffel, J. Chem. Phys. **18**, 1449 (1950).
[15] A. Okazaki, Y. Suemune, and T. Fuchikami, J. Phys. Soc. Japan **14**, 1823 (1959).
[16] T. Nagamiya, K. Yosida, and R. Kubo, *Advances in Physics*, edited by N. F. Mott (Taylor and Francis, Ltd., London, 1955), Vol. 4, p. 1.

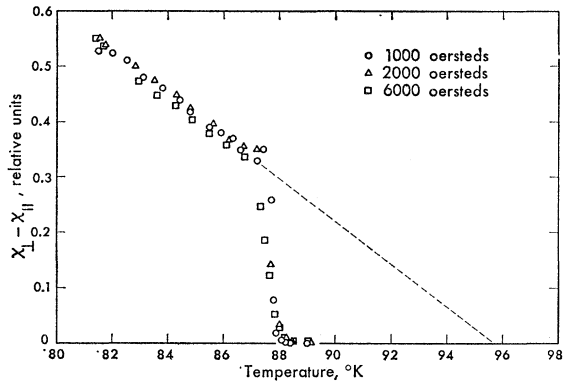


FIG. 3. Plot of $\chi_\perp - \chi_\parallel$ in arbitrary units in the intermediate temperature range.

along a cube edge, discontinuities in the torque appear when the field passes a ⟨100⟩ direction with some hysteresis with respect to the direction of rotation of the magnetic field. One interesting way of demonstrating this behavior is to orient the field along a ⟨100⟩ direction and slowly increase its magnitude. For fields below 7000 oe there is no torque observed. Above a critical field, which is a function of temperature as shown in Fig. 4, a torque suddenly develops and increases linearly with the field for higher values of the field. The linear variation of torque with field and the hysteresis strongly suggest the development of a weak ferromagnetic moment as the result of a large applied field. We will return to a discussion of this field induced transition in Sec. V after examining the behavior at lower temperatures.

Finally, below 81.5° the crystal behaves as if it has a spontaneously developed weak moment. The curves of torque vs angle increase linearly with the field as shown in Fig. 2 and show hysteresis over the whole range of applied fields. The striking feature of the torsion curves is the existence of strong discontinuities in torque. These discontinuities persist down to temperatures in the helium range, where they are most strongly developed. Data for three different suspension directions are shown in Fig. 5. The discontinuities observed along the ⟨100⟩ direction for the magnetic field in a {100} plane tend to disappear at high magnetic fields. At 77°K these discontinuities have pretty well disappeared in fields above 1000 oe. At 4.2° they disappear only above 10 000 oe. The relative amplitudes of the discontinuities vary from crystal to crystal. They even vary for a given crystal with repeated temperature cycling, suggesting that the multiple discontinuities are to be identified with the twinned structure of the crystal.

The linear dependence of the torque on field plus the existence of discontinuities strongly suggests the existence of a weak moment with a number of energetically equivalent directions. There must always be at least two equivalent directions, corresponding to reversal of the sublattice magnetization and therefore of the weak moment. The fact that the discontinuities are present down to very low fields and remain even at high fields suggests that the mechanism involved is antiferromagnetic domain wall motion where the wall is driven by the interaction of the weak moment and the applied field. The small angular hysteresis which is observed at the discontinuities is consistent with this interpretation, with $H\Delta\theta/2$ oe being a coercive field. For very high fields one would expect that domain rotation processes would come in and some of the discontinuities would disappear. This is our interpretation of the softening of the ⟨100⟩ discontinuities at high field. The results described here are very similar to those obtained in the torsion studies of $NiF_2$ and the rare-earth orthoferrites.[17] It has been shown that the $F^{19}$ nuclear resonance in $NiF_2$ can be excited by domain wall motion[18] confirming that this motion is a principal magnetization process. We believe that the wall processes in $NiF_2$ and $KMnF_3$ are entirely similar with the exception that whereas there are four equivalent directions for the weak moment in $NiF_2$,[9] there are as we shall see only two equivalent directions in $KMnF_3$. It is at first sight surprising that the $KMnF_3$ torque does not show strong $H^2$ components at high fields as does the $NiF_2$ torque.[17] This may be partly because the $KMnF_3$ crystals are highly twinned whereas the $NiF_2$ crystals are untwinned. But, in addition, as will be discussed in Sec. V, there are indications of a strong parallel susceptibility at low temperatures in $KMnF_3$. It is not unlikely that the anisotropy in the susceptibility is considerably smaller than in an axial antiferromagnet or in a canted antiferromagnet with high axial anisotropy.

## III. THEORY

In this section we shall study the magnetic structure of $KMnF_3$ from a theoretical point of view. First an approach based only on symmetry analogous to that proposed by Dzialoshinskii[7] in explaining the weak

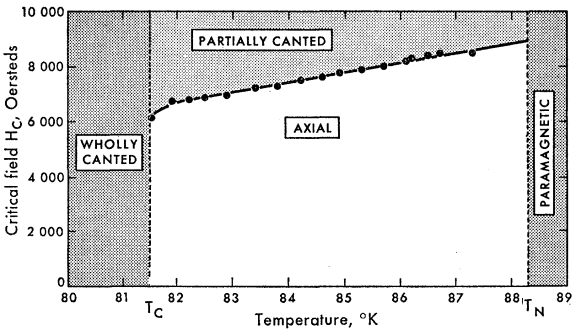


FIG. 4. The critical field at which canting is produced is shown as a function of temperature.

[17] L. M. Matarrese and J. W. Stout, Phys. Rev. **94**, 1792 (1954); R. C. Sherwood, J. P. Remeika, and H. J. Williams, J. Appl. Phys. **30**, 217 (1959); C. Kuroda, T. Miyadai, A. Naemura, N. Niizeki, and H. Takata, Phys. Rev. **122**, 446 (1961).

[18] R. G. Shulman, J. Appl. Phys. **32**, 126S (1961).

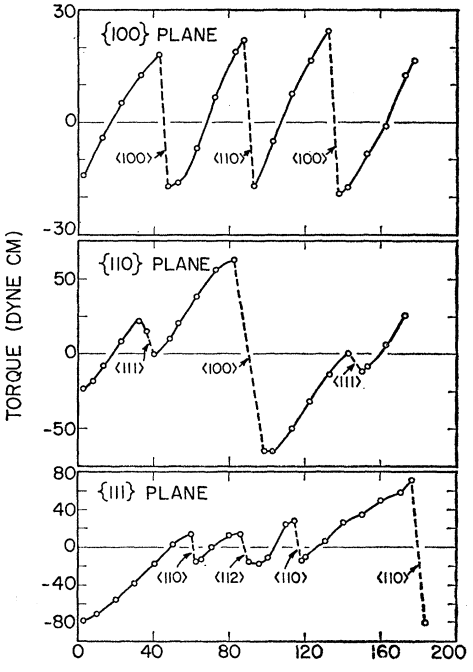


FIG. 5. Magnetic torson measurements in $KMnF_3$ at 4.2°K in a field of 2000 oe. The magnitudes of the discontinuities are proportional to the field. It is believed that the discontinuities arise from domain wall motion as discussed in the text.

ferromagnetism of Fe will be developed. Then we shall give a phenomenological theory based on the lattice distortions as given in I.

Dzialoshinskii has shown that the possible magnetic structures of a given crystal may be derived from symmetry considerations alone. We now apply this theory to $KMnF_3$. The space group of $KMnF_3$ is $Pbnm$ ($D_{2h}^{16}$) where the three twofold rotation axes are all screw axes as shown in Fig. 6. The magnetic state of this crystal can be described by assigning a mean spin function $\mathbf{S}_i$ to each of the four $Mn^{2+}$ ions in the unit cell. Having done this, we expand the thermodynamic potential $\Phi$ in a power series in the components of the $\mathbf{S}_i$. Such an expansion will converge rapidly for temperatures near the Néel point where the $\mathbf{S}_i$ are small. This anisotropy series should converge rapidly even well below $T_N$ since the distortions from cubic symmetry are all very small. The expansion of $\Phi$ can contain only even powers since $\Phi$ must be invariant to replacement of every $\mathbf{S}$ by $-\mathbf{S}$ (time-reversal symmetry). Furthermore, the expansion must be invariant under the operations of the space group of the crystal.

We introduce the vectors $\mathbf{m}$, $\mathbf{l}_1$, $\mathbf{l}_2$, and $\mathbf{l}_3$ defined by

$$\mathbf{m}=\mathbf{S}_1+\mathbf{S}_2+\mathbf{S}_3+\mathbf{S}_4,$$
$$\mathbf{l}_1=\mathbf{S}_1-\mathbf{S}_2+\mathbf{S}_3-\mathbf{S}_4,$$
$$\mathbf{l}_2=\mathbf{S}_1-\mathbf{S}_2-\mathbf{S}_3+\mathbf{S}_4,$$
$$\mathbf{l}_3=\mathbf{S}_1+\mathbf{S}_2-\mathbf{S}_3-\mathbf{S}_4,$$

where the subscripts correspond to the four $Mn^{2+}$ ions in the unit cell as labeled in Fig. 6. As we shall see below, sites 1 and 3, and 2 and 4 are equivalent to the order of our energy expansion. Although the space group allows four sublattices, we will expect only two sublattices in practice. Then $\mathbf{l}_2$ and $\mathbf{l}_3$ will be identically zero and we may simply write $\mathbf{l}_1$ as $\mathbf{l}$.

We now consider the transformation properties of $\mathbf{l}$ and $\mathbf{m}$. The character table for the group $D_2$ is

| | | $E$ | $C_2^z$ | $C_2^y$ | $C_2^x$ |
|---|---|---|---|---|---|
| $D_2$ | $A_1$ | 1 | 1 | 1 | 1 |
| | $B_1$ | 1 | 1 | −1 | −1 |
| | $B_2$ | 1 | −1 | 1 | −1 |
| | $B_3$ | 1 | −1 | −1 | 1 |

We need not consider the full point group $D_{2h}$ since both $\mathbf{m}$ and $\mathbf{l}$ are even under inversion. Now $\mathbf{m}$, being simply the mean magnetic moment per unit cell, transforms like an axial vector. Thus $m_x$ transforms according to $B_3$, $m_y$ according to $B_2$, and $m_z$ according to $B_1$. The minus signs in $\mathbf{l}$ complicate its transformation properties somewhat. From Fig. 6 we see that the screw axes $C_2^z$ and $C_2^x$ take ions labeled by $\oplus$ onto ions labeled by $\ominus$ where the sign given to the $i$th ion corresponds to the sign in front of $\mathbf{S}_i$ in $\mathbf{l}$. $C_2^y$, however, takes a $\oplus$ onto a $\oplus$. Thus $l_z$ transforms according to $B_3$, $l_y$ according to $A_1$, and $l_x$ according to $B_1$.

We are now in a position to write the most general form of the expansion of $\Phi$ in terms of the components of $\mathbf{l}$ and $\mathbf{m}$, including all invariants of second order:

$$\Phi=-\tfrac{1}{2}Al^2+\tfrac{1}{2}Bm^2-\tfrac{1}{2}\alpha l_x^2+\tfrac{1}{2}\beta l_y^2 +\tfrac{1}{2}am_x^2+\tfrac{1}{2}bm_y^2-\gamma m_x l_z-\delta m_z l_x.$$

We have written terms only to second order assuming all higher terms small. The terms in $\Phi$ which are independent of orientation with respect to the crystal axes

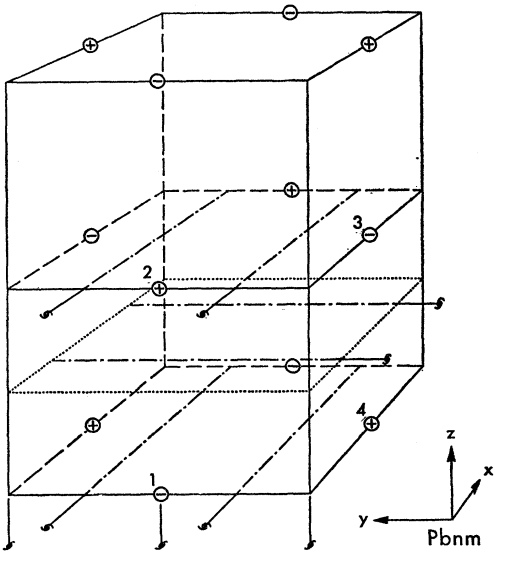


FIG. 6. Location of screw axes with respect to $Mn^{2+}$ ions in $KMnF_3$.

are clearly to be identified with exchange terms, whereas the other terms are of anisotropy origin. Thus the ratio of the coefficients of such terms is of the order of the ratio of the anisotropy energy to the exchange energy and is small.

Minimizing $\Phi$ for a given $\mathbf{l}$ gives the equations

$$\begin{aligned} \alpha l_x+\delta m_z+\mu l_x=0, \quad & (B+a)m_x-\gamma l_z=0, \\ \beta l_y-\mu l_y=0, \quad & Bm_y+bm_y=0, \\ -\gamma m_x-\mu l_z=0, \quad & Bm_z-\delta l_x=0, \end{aligned}$$

where $\mu$ is a Lagrangian multiplier. These equations have the following solutions:

$$\begin{aligned} &\text{(i)} \quad m=0, && l_x=l_z=0, && l_y\neq 0. \\ &\text{(ii)} \quad m_x=+\gamma l_z/(a+B), && l_x=l_y=m_y=m_z=0, \\ &\text{(iii)} \quad m_z=+\delta l_x/B, && l_y=l_z=m_x=m_y=0. \end{aligned}$$

Solutions corresponding to different magnetic ordering will exist corresponding to $l_2$ and $l_3$ not equal to zero. To the order of the expansion given here, these solutions will not mix with the solution corresponding to an alternating magnetic structure. The alternating structure has three possible solutions: Solution (i) corresponds to the sublattice along the + and − $y$ axes with no canting. Solution (ii) corresponds to the sublattice along the + and − $z$ axes and canted so as to produce a magnetic moment along the $x$ axis. Finally solution (iii) corresponds to the sublattice along the + and − $x$ axes and canted so as to produce a weak moment along the $z$ axis.

Since the actual lattice distortions have been determined in I, it is possible to examine the microscopic theory of canting in this structure. The crystal structure is shown again in Fig. 7 with the fluorine displacements shown. We first find the potential in the vicinity of the $Mn^{2+}$ sites as a function of the fluorine displacements. The Mn ion at site 1 is surrounded by six fluorine ions located at

$$\begin{aligned} &\pm[a/2\sqrt{2}+\eta a/\sqrt{2},\ -a/2\sqrt{2}+\eta a/\sqrt{2},\ -\zeta c], \\ &\pm[a/2\sqrt{2}-\eta a/\sqrt{2},\ a/2\sqrt{2}\pm\eta a/\sqrt{2}-\zeta c], \\ &\pm\xi a,0,c/2], \end{aligned}$$

where $\xi$, $\eta$, $\zeta$ are the fluorine displacements shown in Fig. 7. We can reproduce the fluorine distribution about site 2 from the distribution about site 1 by the transformation:

$$\zeta\rightarrow-\zeta \quad \text{and} \quad \xi\rightarrow-\xi.$$

Similarly for site 3: $\eta\rightarrow-\eta$; and for site 4: $\xi\rightarrow-\xi$, $\eta\rightarrow-\eta$, $\zeta\rightarrow-\zeta$. We write the potential about site 1 to second order in the distances from site 1 and to first order in the lattice distortions:

$$V_1=12(9/a)[1-(\psi/3)+2\psi(r^2-3z^2)/a^2+8xz\mathcal{E}/a^2]$$

where $\psi=(c/a)-1$ and $\mathcal{E}=(\xi-\sqrt{2}\zeta)$. We now write the single-ion anisotropy energy as an expansion in powers of the spin components. Since the anisotropy energy should transform in the same way as the potential, we expect

$$\begin{aligned} \Phi_1=\Phi_3&=+(D\psi/4)[S(S+1)-3S_z^2]+D\mathcal{E}S_xS_z, \\ \Phi_2=\Phi_4&=+(D\psi/4)[S(S+1)-3S_z^2]-D\mathcal{E}S_xS_z, \end{aligned}$$

where we have used the relation between the distortions as viewed from the various sites. In what follows it will be convenient to write the magnetic energy per unit volume in terms of the sublattice magnetizations

$$\mathbf{M}_1=Ng\mu_B\mathbf{S}_1/2 \quad \text{and} \quad \mathbf{M}_2=Ng\mu_B\mathbf{S}_2/2.$$

where we have assumed that $\mathbf{S}_1=\mathbf{S}_3$ and $\mathbf{S}_2=\mathbf{S}_4$ since their anisotropies are equal. We write for the total magnetic energy per mole

$$\begin{aligned} \mathcal{H}=+\lambda\mathbf{M}_1\cdot\mathbf{M}_2&-K_1(M_{1z}^2+M_{2z}^2)/2M^2 \\ &-K_2(M_1^xM_1^z-M_2^xM_2^z)/M^2. \end{aligned}$$

We may now find the positions of minimum energy subject to the constancy of the sublattice magnetization. We obtain three solutions:

$$\begin{aligned} \text{(i)} \quad & M_1^x=M_2^x=0, \\ & M_1^y=-M_2^y=M, \\ & M_1^z=M_2^z=0, \\ & U=-\lambda M^2; \\ \text{(ii)} \quad & M_1^y=M_2^y=0, \\ & M_1^x=M_2^x\sim K_2/2\lambda M, \\ & M_1^z=-M_2^z\sim M, \\ & U=-\lambda M^2-K_1-K_2^2/\lambda M^2; \end{aligned}$$

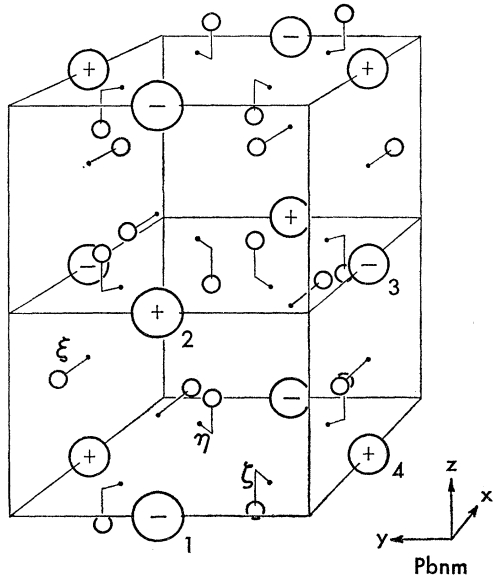


FIG. 7. Flourine distortions in $KMnF_3$.

(iii) $M_1^y = M_2^y = 0$,

$M_1^z = M_2^z \sim K_2/2\lambda M$,

$M_1^x = -M_2^x \sim M$,

$U = -\lambda M^2 - K_2^2/\lambda M^2$.

We see as expected from the general group theoretical arguments that there are two solutions with a canted magnetization and one solution with an uncanted magnetization. Solution (ii) is lowest with solution (iii) next and the uncanted solution highest in energy presuming that $K_1$ is positive.

## IV. INTERPRETATION OF LOW-TEMPERATURE BEHAVIOR

In this section we compare the torsion behavior below 81.5°K with that expected from the theory of the effect of lattice distortion on the magnetic structure. The observed fluorine distortions are given in Table I. We observe from the table that at 95°K, which is above the Néel point, the fluorine octahedra are orthorhombically distorted. At the Néel point [11] the $c/a$ ratio drops below one and the fluorine distortion becomes tetragonal. Finally at 65°K, which is below the lower transition, the fluorines are again distorted orthorhombically.

TABLE I. X-ray strain parameters.

| $T$(°K) | $\xi$ | $\eta$ | $\zeta$ | $\psi$ | $\varepsilon$ |
|---|---|---|---|---|---|
| 65 | 0.050 | 0.042 | 0.060 | −0.002 | −0.035 |
| 84 | 0.054 | 0.025 | 0.036 | −0.002 | +0.003 |
| 95 | 0.032 | ··· | 0.068 | +0.006 | −0.064 |

In this section we first discuss the positions of the discontinuities observed in the torsion, and then their magnitude, which is an indication of the size of the weak moment. The discontinuities should occur when the applied field makes equal angles with the two degenerate directions for the weak moment. Therefore we expect the following discontinuities on the basis of the theoretical results of Sec. III.

1. Sample suspended along a cube edge should give discontinuities for state (ii) when the field passes ⟨110⟩ directions and ⟨100⟩ directions. For state (iii) the weak moment should reverse when the field passes ⟨100⟩ directions.

2. Sample suspended along a face diagonal should give discontinuities for state (ii) when the field passes ⟨100⟩ directions and ⟨111⟩ directions. For state (iii) the weak moment should reverse when the field passes ⟨110⟩ direction and ⟨100⟩ directions.

3. Sample suspended along a body diagonal should give discontinuities for state (ii) when the field passes ⟨110⟩ directions and ⟨112⟩ directions. For state (iii) the weak moment should reverse when the field passes ⟨110⟩ directions.

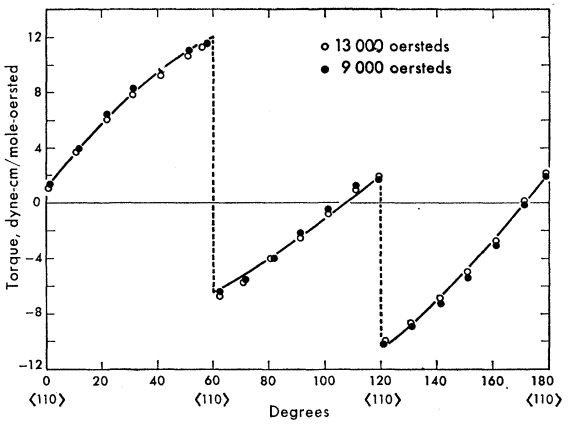


FIG. 8. Torque per unit field as a function of the angle of the field from a ⟨110⟩ direction for the field in a {111} plane. The closed points are for 9000 oe and the open points are for 13 000 oe.

Comparison of the data as described in Sec. II shows that the discontinuities do occur at these positions and only at these positions. Since all the expected discontinuities actually appear we must conclude that both states (ii) and (iii) are present. However those discontinuities associated with state (ii) are always relatively small and sometimes absent altogether. This suggests that state (iii) may have the lower energy. A theoretical fit of the torsion data is shown in Fig. 8 for the sample suspended along a ⟨111⟩ direction with only state (iii) present. We can use the data to determine the strength of the weak moment by the following argument. The torque as a function of angle can be written as

$$\tau = H\, M\cos\theta_0(f_1 \sin\theta_1 + f_2 \sin\theta_2 + f_3 \sin\theta_3),$$

where $\theta_0 = \cos^{-1}[(2/3)^{\frac{1}{2}}]$ is the angle between the $z$ axis and the ⟨111⟩ plane, and $\theta_1$, $\theta_2$, and $\theta_3$ are the angles between the applied field and the projections of the $z$ axes of the three kinds of crystallites onto the ⟨111⟩ plane. The relative fractions of each crystallite present are indicated by $f_1$, $f_2$, and $f_3$. From ratios of the magnitudes of the discontinuities we can determine $f_1$, $f_2$, and $f_3$. Finally we determine the weak moment at 4.2°K to be

$$m = 19.3 \text{ emu/mole},$$

where the sublattice magnetization $M = 14\,000$ emu/mole. Then the anisotropy constant per mole at 4.2°K is

$$K_2 = \lambda M m = 1.8\times10^7 \text{ ergs/mole}.$$

The single-ion anisotropy energy is

$$D\mathcal{E} = -2K_2/NS^2 = -9.6\times10^{-18} \text{ ergs/ion}.$$

The weak moment has similarly been determined at 77°K and found to be equal to 0.77 emu/mole. On the assumption of molecular field theory we expect the magnetization to be given by the associated Brillouin function:

$$M(T) = M(0)B_{\frac{5}{2}}(T).$$

Then the magnetization at 77°K should be 0.5 times the saturation value. This gives $K_2(77°\text{K})=4.5\times10^5$ ergs/mole or about a factor of 40 smaller than the value at 4.2°K. On the assumption that $K_2$ varies as the third power of the magnetization as suggested by spin-wave arguments[19] we would expect a reduction by only a factor of 8. Evidently the apparent moment is more strongly temperature dependent than expected from these arguments. On the assumption that the strain at 4.2°K is the same as at 65°K we compute for the single-ion anisotropy constant

$$D=2.7\times10^{-16}\text{ ergs/ion (experimental).}$$

This value is to be compared with Pearson's computed value[12] of

$$D=1.6\times10^{-16}\text{ ergs/ion (theoretical).}$$

With the uncertainties in the calculation and some question about the fluorine distortion at low temperatures, this agreement seems quite satisfactory and supports the idea that the anisotropy arises from a distortion of the manganese $3d$ wave functions.

## V. INTERPRETATION OF INTERMEDIATE-TEMPERATURE BEHAVIOR

The presence of a state with no weak moment intermediate between the low-temperature canted phase and the high-temperature paramagnetic phase is puzzling. From the arguments of Sec. III one would be inclined to think that the sublattice magnetization must be directed along the $y$ axis, which is a pseudocell ⟨110⟩ direction in this intermediate temperature range. However, the torsion data of Fig. 1 unambiguously establishes that the magnetization is directed along a pseudocell ⟨100⟩ direction. We are therefore forced to the conclusion that $K_2$ is identically zero in this intermediate temperature range. As may be seen from Table I, whereas $\mathcal{E}$ is large and negative both above 88.3°K and below 81.5°K it is small and probably zero to within experimental error in the intermediate temperature range. The perovskite structure is highly unstable and we can only presume that the contraction of the $c$ axis at the Néel point stabilizes the fluorine octahedron with $\mathcal{E}=0$. We then imagine that at the Néel point the free energy of the canted state is higher than the free energy of the uncanted state by an amount $\Delta\Phi$. As the temperature is lowered, the free energy of the canted state drops with respect to that of the uncanted state because of the canting energy. The free energy may also drop if the exchange coupling in the canted state is higher, but we do not consider that possibility. We can expect that at the temperature at which these two terms are equal, we will obtain a transition to the canted state:

$$\Delta\Phi=-K_2^2(T_c)/\lambda M^2(T_c)+\Delta\Phi_L(T_c)=0.$$

From the liquid-nitrogen data this result suggests that the free-energy difference is only 60 ergs/mole. For reference the shear modulus of an ionic crystal like NaCl is $3.5\times10^{12}$ ergs/mole. With 3% distortion the shear energy would be $2\times10^9$ ergs/mole. Evidently the fluorines are extremely free to distort in the perovskite structure.

As was remarked earlier, another surprising feature of the intermediate state is that the sublattices cant under the application of a large magnetic field. This observation suggests that a static applied field lowers the free energy of the canted state so that this state becomes stable. Orbach[20] has noticed that the parallel susceptibility of a canted antiferromagnet at $T=0$ is equal to

$$\Delta\chi(0)=(K_2/\lambda M^2)(K_2/K_1)/2\lambda,$$

whereas it is zero for an uncanted antiferromagnet. At finite temperature we find that the parallel susceptibility will be increased on canting by an amount

$$\Delta\chi(T)=\Delta\chi(0)[1-\chi_{11}(T)K_1/4M^2].$$

In a structure where $K_2$ is very much larger than $K_1$, as is the case here, this increase in susceptibility may be considerable. Then the critical field for canting at temperature $T$ will be given by

$$\Delta\Phi=-K_2^2(T)/\lambda M^2(T)+\Delta\chi(T)H_c^2(T)/2+\Delta\Phi_L(T)=0.$$

We obtain then for the square of the critical field, under the assumption that $\Delta\Phi_L(T)$ and $\Delta\Phi_L(T_c)$ are equal:

$$H_c^2(T)=4\lambda K_1(T)\frac{M^2(T)}{K_2^2(T)}\left[\frac{K_2^2(T_c)}{M^2(T_c)}-\frac{K_2^2(T)}{M^2(T)}\right].$$

From molecular field theory we expect for an Ising antiferromagnet the temperature dependence of the magnetization close to the Néel temperature $T_N$ will be given by

$$M^2(T)=3M^2(0)(T/T_N)^2(T_N-T)/T_N.$$

We will also expect in this region that the anisotropy in the canted state $K_2(T)$ will vary as the square of the magnetization. Under these assumptions we obtain

$$H_c(T)=[4\lambda K_1(T)]^{\frac{1}{2}}[(T-T_c)/(T_N-T)]^{\frac{1}{2}}.$$

We expect the axial anisotropy to be given by

$$K_1(0)=-\tfrac{3}{4}D\psi NS^2=1.1\times10^6\text{ ergs/mole,}$$

where we have used the experimental anisotropy constant. The temperature dependence of the axial anisotropy in the intermediate phase has been determined directly from antiferromagnetic resonance[21] and is given by

$$K_1(T)=1.4\times10^6(T_N-T)/T_N\text{ ergs/mole.}$$

[19] P. Pincus, Phys. Rev. **113**, 769 (1959).

[20] R. Orbach, Phys. Rev. **115**, 1189 (1959).

[21] A. J. Heeger, A. M. Portis, and Dale T. Teaney (to be published).

We then expect on the assumption that only canting energy is involved that the critical field will be given by

$$H_c(T)=2.0\times10^4[(T-T_c)/T_N]^{\frac{1}{2}} \text{ oe.}$$

This equation gives for the critical field at $T=T_N$:

$$H_c(T_N)=6000 \text{ oe,}$$

which is in moderate agreement with the observed value of about 9000 oe. Should the fluorine distortion also increase the strength of the exchange coupling we would then underestimate $\Delta\Phi_L$ and therefore compute too small a critical field. Since the square of the observed critical field is only twice what we calculate, the increased exchange energy is at most comparable to the canting energy. A second possibility is that $\Delta\Phi_L$ is strongly temperature dependent in this range, changing by a factor of 2 between $T_c$ and $T_N$, but this seems unlikely.

There is one important difference between the canting transition as induced by a magnetic field and the canting transition as induced by reducing the temperature. When the field is raised above the critical field and along a (100) direction, we can expect that only those crystallites with $c$ axes along the particular (100) direction will cant. On the other hand, when the temperature is lowered below 81.5° all crystallites will cant. If the sample is cooled in a large field, one expects that about $\frac{1}{3}$ of the crystallites will be canted in the intermediate temperature range and that the other $\frac{2}{3}$ will cant at the critical temperature. This distinction bears on possible hysteresis of the transition temperature. While we observe no hysteresis associated with the critical field in the intermediate-temperature range, we do observe a large hysteresis associated with the thermally induced canting. By examining the torque in a small magnetic field it is observed that, on warming, a weak moment may persist up to as high as 83.5°K as shown in Fig. 9. From the fact that there is no hysteresis in the field induced canting and since this is presumably a first-order transition, we must conclude that the transition is nucleated in both directions. Since the transition for thermally induced canting is very nearly the temperature at which the critical field goes to zero, it would appear that canting is also nucleated on cooling. On the other hand, there is a marked hysteresis on warming which suggests that there is no substantial nucleation of the axial structure once the whole crystal is canted.

The transition at 81.5°K from the uncanted to the canted state has the general properties of a Jahn-Teller effect where the lattice distorts and removes a magnetic degeneracy. In this case the distortion removes the degeneracy of the dispersion relations for the normal modes of a simple antiferromagnet.

We finally discuss the antiferromagnetic transition itself. The sharp reduction in the $c$ axis at the Néel point[11] and the very sudden increase in the anisotropy in the susceptibility shown in Fig. 3 suggests a first-order

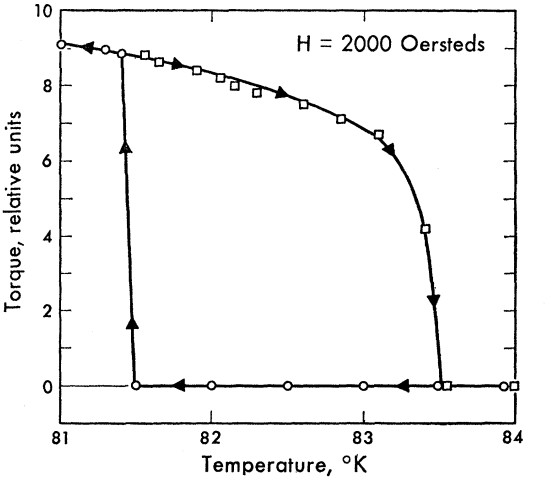


FIG. 9. Torque for the magnetic field along a ⟨100⟩ direction on cooling and on heating. These data suggest that the phase transition to a canted structure is nucleated on cooling. The transition on heating takes place only when the canted state is unstable.

transition. Bean and Rodbell[22] have shown that if the exchange constant is a sufficiently sensitive function of lattice strain the disordering transition may be first order. If we characterize the state of the crystal by the single strain parameter $\psi=c/a-1$, we may write for the free energy

$$\Phi=\tfrac{1}{2}c(\psi-\psi_0)^2-\lambda[1-\beta(\psi-\psi_0)]M^2-TS.$$

For an Ising antiferromagnet we obtain, by minimizing the free energy with respect to both lattice strain and magnetization:

$$M=M_0\tanh(T/T_N)[1+(b/3)(M/M_0)^2],$$

where

$$kT_N=\lambda M_0^2/N \quad \text{and} \quad b=3\beta^2\lambda M_0^2/c.$$

As long as $b$ is less than unity, the transition at the Néel point is second order with the magnetization a continuous function of temperature. But for $b$ slightly larger than unity, the magnetization jumps discontinuously at the Néel point to a value

$$M(T_N)\sim M_0[5(b-1)/3]^{\frac{1}{2}}.$$

The lattice strain is related to the magnetization and is given by

$$(\psi-\psi_0)=-(b/3\beta)(M/M_0)^2.$$

We then expect for a first-order transition that the discontinuity in the strain at the Néel point will be given by

$$\Delta\psi\sim-(5/9\beta)b(b-1).$$

As the system cools, the magnetization grows toward $M$ and the strain approaches a maximum value at $T=0$ of

$$\psi(0)=\psi_0-b/3\beta.$$

[22] C. P. Bean and D. S. Rodbell, Bull. Am. Phys. Soc. **6**, 159 (1961).

In the absence of a strain dependence of the magnetization, we would have near the Néel point

$$(M/M_0)^2=3T^2(T-T_N)/T_N^3.$$

We can view the problem with strain as being characterized by a strain-dependent Néel temperature:

$$T_0=T_N[1-\beta(\psi-\psi_0)].$$

Then as the magnetization increases the apparent Néel temperature also increases so that the square of the magnetization will grow faster than linearly with the temperature.

This theory seems to give an adequate description of the transition with numerical constants of a reasonable order of magnitude. There are two features of the theory which are not observed, however. The crystal should continue to strain as the temperature is lowered, and no such additional strain is observed. Also the data of Fig. 3 suggest a linear variation in the square of the sublattice magnetization, indicating that there is no variation in the exchange constant below the transition. These two observations are consistent with each other and indicate that terms in the strain energy of higher than second order must be considered. Rather than attempt to describe the lattice energy by a power series in the strain, a physical description will be adequate for our purposes. We imagine that the elastic constant $c$ for small strains $\psi-\psi_0$ is sufficiently small that the magnetic transition is first order with a discontinuity in the strain $\Delta\psi$. As the temperature is lowered there is an additional strain over a few tenths of a degree. Higher-order terms then substantially limit the strain so that there is no further increase in exchange constant as the temperature is lowered. The linear extrapolation of the data of Fig. 3 indicates an apparent Néel temperature

$$T_0=95.6°\text{K}.$$

From the x-ray data[11] we know that $\psi(0)-\psi_0=0.008$ so that we obtain for the strain dependence of the exchange

$$\beta=(1/T_N)dT_0/d\psi=10.8.$$

This value is about equal to the strain dependence of the repulsive energy and seems physically reasonable. It is also about equal to the value required to account for exchange-inversion transitions.[23]

From the data of Fig. 3 we conclude that the discontinuity in the magnetization at the transition is at most about 30%. Then $(b-1)$ is at most about 0.05 at the transition. The elastic stiffness constant for axial strain will then be given by

$$c=3\beta^2\lambda M_0^2/b\sim 4.6\times 10^{12}\text{ ergs/mole}.$$

This value is of the order of magnitude obtained in ionic crystals and does not seem unreasonable. Actually the data of Fig. 3 do not have sufficient resolution to establish beyond question that the transition is of first order. One could have a value of $b$ just below unity but sufficiently close to give a rapid but continuous increase in magnetization. What seems to establish the antiferromagnetic ordering transition as a first-order transition is the hysteresis observed on warming. Although there is no noticeable magnetic hysteresis, the crystal transforms to an orthorhombic phase with three different axes.[11] This phase is stable up to about 15° above the Néel point.

## ACKNOWLEDGMENTS

We have benefited from discussions with Professor F. Keffer concerning the origin of anisotropy in this structure. Dr. R. J. Elliott and Professor C. Kittel have made a number of helpful comments concerning magnetoelastic transitions. Discussions with Dr. Dale T. Teaney on the resonance behavior in the intermediate temperature range are gratefully acknowledged.

[23] C. Kittel, Phys. Rev. **120**, 335 (1960).